# Analysis of the Repulsive Permanent Magnetic Levitation Mechanism and Its Dynamic Behavior

[1]Omar Haddad, [2] Elie Mansour,[3]Jad Chahine
[1,2,3]Department of Mechanical Engineering
[1,2,3]Arts, Sciences and Technology University in Lebanon

**Abstract: This study investigates the repulsive permanent magnetic levitation (PML) mechanism and its dynamic characteristics. The PML system, which utilizes the repulsive forces between permanent magnets, offers potential applications in fields such as transportation, precision engineering, and robotics. The primary aim of this research is to analyze the key factors influencing the stability, response, and dynamic behavior of the levitation system. By employing a combination of theoretical modeling, numerical simulations, and experimental validation, the study explores the relationship between magnetic force, levitation height, and system dynamics. The dynamic characteristics of the system, including the natural frequencies, damping ratios, and response to external disturbances, are thoroughly examined. The results demonstrate how various parameters, such as magnet configuration, material properties, and external forces, impact the system's overall performance. This work provides valuable insights into the optimization of repulsive PML systems, contributing to the development of more efficient and stable levitation technologies.**

**Keywords: Repulsive permanent magnetic levitation, dynamic characteristics, system stability, magnetic force, levitation height, natural frequencies, damping ratios, numerical simulations, experimental validation, optimization.**

## 1. Introduction:

The concept of magnetic levitation has garnered significant attention in recent decades due to its potential applications across a wide range of industries, from transportation to high-precision manufacturing and robotics. Among the various magnetic levitation systems, repulsive permanent magnetic levitation (PML) stands out as a promising technology due to its unique ability to achieve stable levitation without the need for external power sources or complex control systems. This form of levitation utilizes the repulsive forces between permanent magnets to counteract the force of gravity, allowing for contactless support and reduced friction, which leads to advantages such as increased efficiency, reduced wear and tear, and enhanced stability.

The dynamics of repulsive PML systems, however, are complex and depend on various factors, including the configuration and alignment of the magnets, material properties, and the influence of external forces such as vibrations and disturbances. Unlike electromagnetic levitation systems, which require active feedback mechanisms to maintain stability, PML systems rely on the natural repulsive force between the magnets. While this passive nature offers many benefits, it also introduces challenges in terms of achieving stable levitation and maintaining desired dynamic characteristics.

Understanding the dynamic behavior of repulsive PML systems is crucial for optimizing their design and performance. This includes exploring the effects of magnet geometry, levitation height, and the interaction between magnetic fields on the system's response to external perturbations. The primary goal of this study is to provide a comprehensive analysis of the dynamic characteristics of repulsive permanent magnetic levitation mechanisms. This involves developing theoretical models, performing numerical simulations, and conducting experimental investigations to better understand the relationship between system parameters and their impact on stability, vibration modes, and overall performance.

By examining the key factors that influence the dynamics of repulsive PML systems, this research aims to contribute to the advancement of levitation technologies, providing valuable insights for the development of more stable, efficient, and practical systems. The findings of this study could be particularly relevant for applications in transport systems like maglev trains, where high stability and low energy consumption are critical, as well as in precision

machinery and robotics, where even minute variations in levitation height and stability can significantly impact performance.

In the following sections, we present a detailed exploration of the theoretical foundations of repulsive PML, followed by an analysis of the system's dynamic characteristics through simulations and experimental validation. This study aims to bridge the gap between theoretical understanding and practical implementation, offering a pathway toward more effective and reliable magnetic levitation systems.

**2. Levitation Force Model:**

In the context of Halbach array-based permanent magnetic levitation systems, understanding the levitation force and its relationship with structural parameters such as magnet performance and the levitation gap is crucial for optimizing the system's efficiency and carrying capacity. The red rail R&D team, led by Jiang et al., developed a repulsive levitation frame using Halbach arrays and derived mathematical models for the levitation force from three sets of Halbach array configurations. Their simulation and experimental results demonstrated that a five-group Halbach array repulsive levitation structure outperforms the three-group structure in terms of levitation efficiency and load-bearing capacity.

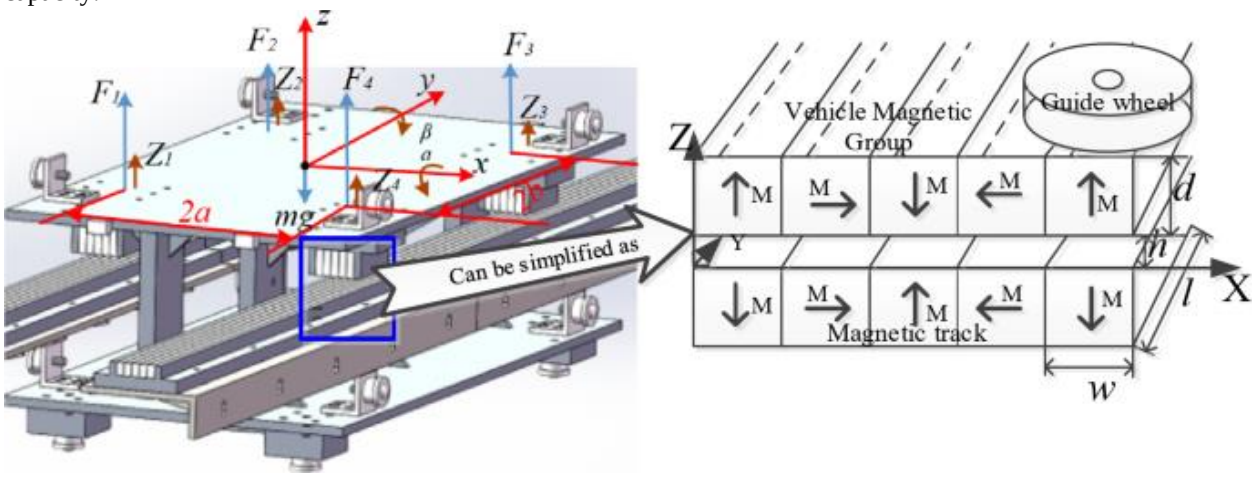


Figure1: Permanent magnetic levitation struct.

In engineering applications, permanent magnet levitation systems are often supplemented with mechanical guide wheels to introduce frictional damping and ensure stability by guiding the levitation system. This enhancement is typically done to achieve self-stabilized levitation. To improve on this, we propose using a five-group Halbach array repulsive levitation structure and establishing its corresponding levitation force mathematical model, as depicted in Fig. 1.

The magnetic induction of the reinforced side of the Halbach array permanent magnet group can be expressed as follows: $B_0$ represents the magnetic induction intensity on the reinforced side, while $B_x$ and $Bz$ represent the components of the magnetic induction along the X and Z axes, respectively. Other parameters include Br, the remanent magnetization of the permanent magnet; k, the number of wavelengths of the Halbach array magnetic group; and λ, the wavelength of the permanent magnet. Additionally, n represents the number of magnetic blocks per unit wavelength, z refers to the levitation air gap, w is the width of the unit magnetic block, and d is the thickness of the permanent magnet. The correction factors $k_1$ and $k_2$ adjust for the magnetic induction intensity. According to prior literature, the levitation force along the Z-axis of the reinforced side of a single levitation module when λ is the wavelength can be expressed as follows:

The levitation force F of the parallel Halbach module is given by:

F=Levitation force along z-axisF = \text{Levitation force along z-axis}F=Levitation force along z-axis

Where the term F represents the levitation force, and LLL represents the length of the vehicle magnet in the Y-axis direction. This equation establishes the connection between the spatial dimensions of the symmetric Halbach levitation structure and the levitation force.

By introducing the proportional correction coefficient $k_1$ and the exponential correction coefficient $k_2$ for the magnetic field strength, and combining them with analog simulation and physical measurements to determine the values of

these coefficients, the model's accuracy and reliability are significantly improved. This adjustment ensures that the analytical model of the levitation force aligns closely with real-world measurements.

To compare the pre-correction and post-correction models, Table 1 presents relevant model parameters. When compared to the original uncorrected model proposed in earlier literature, the inclusion of the correction factors $k_1$ and $k_2$ in the improved model increases its accuracy. Specifically, the proportional correction factor compensates for material property differences among various permanent magnets, while the exponential correction factor accounts for mounting accuracy fluctuations. These refinements enable the model to be adaptable to a wide range of operating conditions, ensuring its robustness and versatility.

The levitation force model is further expanded using the Taylor series method to linearize the equation and simplify the analysis. Higher-order terms are omitted, leading to the following linearized levitation force expression:

**Equation**

The linearized levitation force is expressed as:

$$Fn = Fn(z0)F\_n = F\_n(z_0)Fn = Fn(z0)$$

Where $F_n$ represents the levitation force at various positions, and $F_n(z_0)$ corresponds to the force at the equilibrium point.

The next equation, **Equation (4)**, provides a further refinement of this model, taking into account the balance between forces at different points of the system's operation.

These mathematical models, along with the correction factors and Taylor series expansion, provide a comprehensive framework for understanding and predicting the performance of the Halbach array-based permanent magnetic levitation system, ensuring its practical applicability and optimization for real-world scenarios.

**Stability and decoupling analysis**

In order to analyze the stability of the system and the coupling relationship between the four magnetic poles, the dynamical equations of the system are determined by establishing the coordinate change relationship between the vertical displacement of the four magnetic poles and the displacement and inclination of the three-degree-of-freedom motions, and associating them with the dynamical equations of the system. On this basis, the stability and coupling relationship of the system are analyzed.

According to Fig. 3, the coordinate variation schematic diagrams of the bogie pitching motion and side tilting motion can be drawn, as shown in Fig. 4.

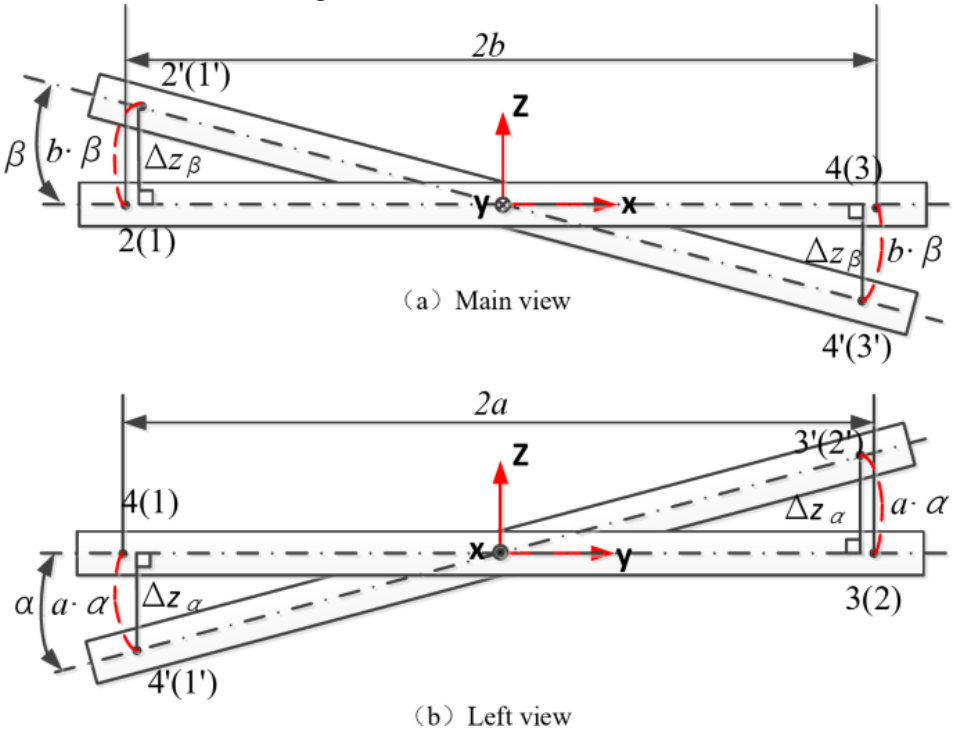


（a）Main view

（b）Left view

Figure2: Schematic diagram of magneto-polar coordinate transformation.

As shown in Fig. 4(a), when the lateral inclination angle of the levitated platform clockwise around the y-axis is β, the magnetic pole 1 moves from point 1 to point 1′, and its arc trajectory length is $b \cdot \beta$, and the vertical displacement

In addition, when the overall vertical displacement of the levitated platform is z, the vertical displacement of pole 1 will be As shown in Fig. 3, when the counterclockwise pitch angle of the bogie around the x-axis is α, magnetic pole 1 moves from point 1 to point 1′, and the length of its arc trajectory is $a \cdot \alpha$, while its vertical displacement is

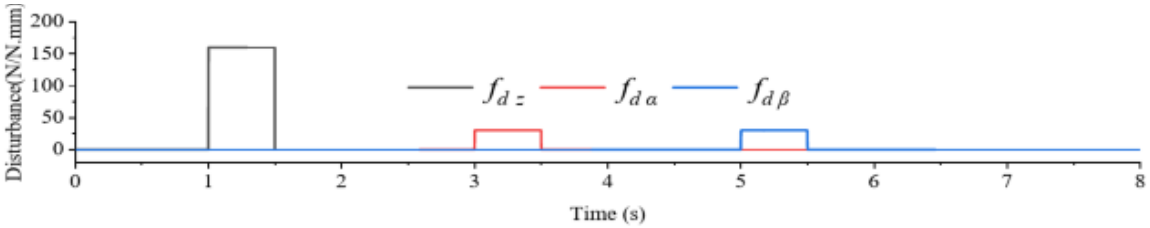


(a) Perturbations in three degrees of freedom

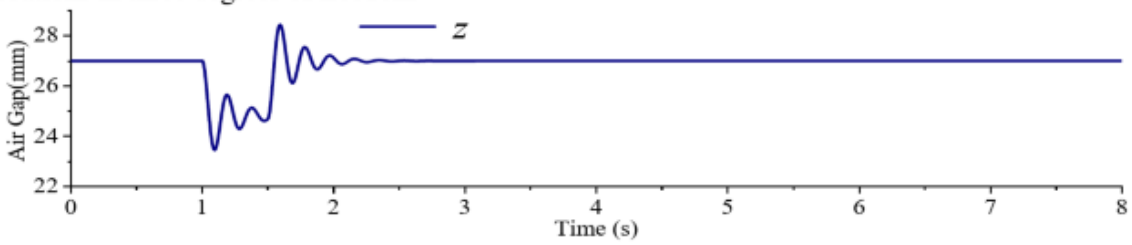


(b) Vertical displacement waveform

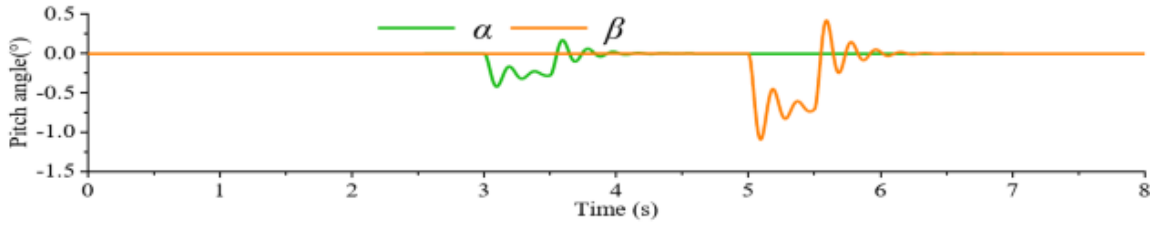


(c) Waveforms of pitch angle $\alpha$ and lateral inclination angle $\beta$

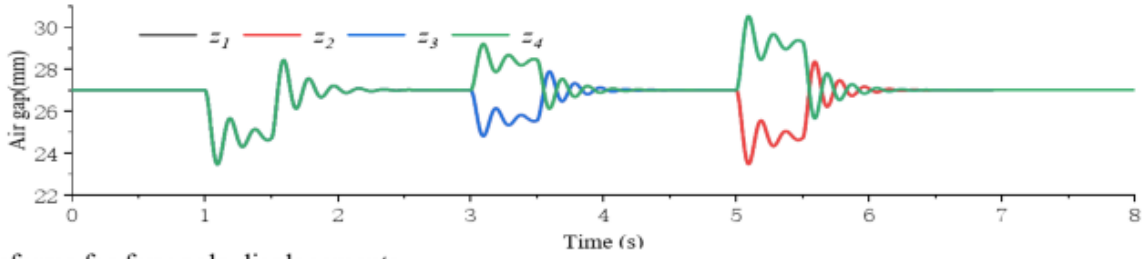


(d) Waveforms for four pole displacements

Figure3: Input–output decoupling simulation waveforms.

**3.Simualtion Results**

To analyze the dynamic characteristics of the repulsive permanent magnetic levitation system, the system is transformed into a second-order, three-input, three-output model. In this model, three variables, x1x_1x1, x2x_2x2, and x3x_3x3, are considered as the system inputs, while the vertical displacement zzz, pitch angle α\alphaα, and lateral inclination β\betaβ are the outputs. The state-space equations for this system are derived using the state variables, leading to the system representation in the following equations:

State-space input-output relationship

State variable representation

First-order state variables

State-space equation

In Equation (19), the matrices AAA, BBB, and CCC represent the system state matrix, input matrix, and output matrix, respectively. These matrices are further defined in Equations (20) and (21).

Substituting the relevant model parameters from Table 2 into Equation (18), a simulation of the dynamic characteristics of the bogie is performed, consisting of the following four steps:

Step 1: Input–Output Decoupling Verification

To verify the decoupling of the input and output variables in the bogie system, step perturbation signals are applied to the system at specific times (1 s, 3 s, 5 s), with perturbation durations of 0.5 s. The amplitude of the vertical

perturbation is 160 N, and the perturbations in the pitch and lateral inclination directions are 30 N·mm each. The displacement zzz, pitch angle α\alphaα, and lateral inclination β\betaβ of the bogie, along with the air gap data from the four magnetic poles, are monitored.

As shown in Fig. 5, the system shows no perturbation during the 0-1 s period, with the initial conditions of z= $27z = 27z = 27\ mm, \alpha = 0 \circ \backslash alpha = 0\hat{}\backslash circ\alpha = 0 \circ, and\ \beta = 0 \circ \backslash beta = 0\hat{}\backslash circ\beta = 0 \circ$. At 1 s, a vertical step perturbation of 160 N is applied for 0.5 s, causing only vertical displacement zzz to oscillate, reaching a minimum of 26.42 mm, while α\alphaα and β\betaβ remain unaffected. At 3 s, a perturbation of 30 N·mm in the pitch direction is applied, causing only α\alphaα to oscillate, and at 5 s, a 30 N·mm perturbation in the lateral inclination direction affects only β\betaβ.

The simulation results confirm that input-output decoupling can be achieved in this system through a coordinate transformation method, as the vertical displacement, pitch angle, and lateral inclination can be independently controlled by applying perturbations at different points in time.

Step 2: Magnetic Pole Perturbation Analysis

To investigate the effects of perturbations at different magnetic poles on the dynamic characteristics of the bogie, perturbations with an amplitude of 16 N are applied to each of the four magnetic poles at 1 s, 3 s, 5 s, and 7 s. The displacement zzz, pitch angle α\alphaα, and lateral inclination β\betaβ, as well as the air gap data for each magnetic pole, are recorded.

The results, shown in Fig. 6, reveal that while the oscillation frequencies of α\alphaα and β\betaβ are the same when perturbations are applied to the four poles, the oscillation amplitude of β\betaβ is generally larger than that of α\alphaα. For example, during the 1-3 s period, when only magnetic pole 1 is perturbed, a small oscillation in zzz is observed, and after about 1.2 s, it stabilizes, while α\alphaα and β\betaβ oscillate around zero. The air gaps of the magnetic poles also change in response to the perturbation, with the largest oscillation occurring at the pole with the initial perturbation, followed by the other poles in decreasing order of amplitude.

Step 3: Simulation Analysis Under Multiple Magnetic Pole Perturbations

To explore the system's behavior under more complex perturbations, step perturbations are applied to the four magnetic poles at different times, as shown in Fig. 7. The resulting dynamic behavior of the bogie is analyzed based on the changes in vertical displacement zzz, pitch angle α\alphaα, and lateral inclination β\betaβ.

During the 1-2 s period, a perturbation is applied only to magnetic pole 1. The system experiences a slight decrease in zzz, which then oscillates and stabilizes at 26.95 mm. The pitch angle α\alphaα increases slightly and oscillates to stabilize at 0.1°, while the lateral inclination β\betaβ decreases and stabilizes at -0.5°. The oscillations of the air gap data follow a similar pattern.

In the 2-3 s period, perturbations are applied to both magnetic poles 1 and 2. The vertical displacement zzz drops initially and then oscillates before stabilizing at 26.9 mm. The pitch angle α\alphaα and lateral inclination β\betaβ oscillate and stabilize at 0° and -1°, respectively. The oscillation amplitudes of the magnetic poles' air gaps follow a similar order of magnitude as in Step 2.

During the 3-5 s period, when only magnetic pole 2 is perturbed, the system behavior is similar to earlier steps. Vertical displacement zzz oscillates slightly around 27 mm, and both pitch angle α\alphaα and lateral inclination β\betaβ stabilize at 0°. The air gaps at the different magnetic poles show the same oscillation patterns, with the largest oscillations observed at the pole closest to the perturbation.

Step 4: Complex Perturbation Simulation

The system's dynamic response to a combination of perturbations at different magnetic poles is explored in this final step. The complex interactions between the four magnetic poles lead to oscillations in all three degrees of freedom (vertical displacement, pitch angle, and lateral inclination). The displacement and air gap oscillations are found to follow patterns similar to the ones observed in earlier steps, with varying amplitudes depending on the perturbation location.

The simulation results highlight the complex interplay between the magnetic pole perturbations and the system's dynamic characteristics. These results provide valuable insights into the behavior of the repulsive permanent magnet levitation system under both single and multiple perturbations, contributing to the understanding of its stability and performance in practical applications.

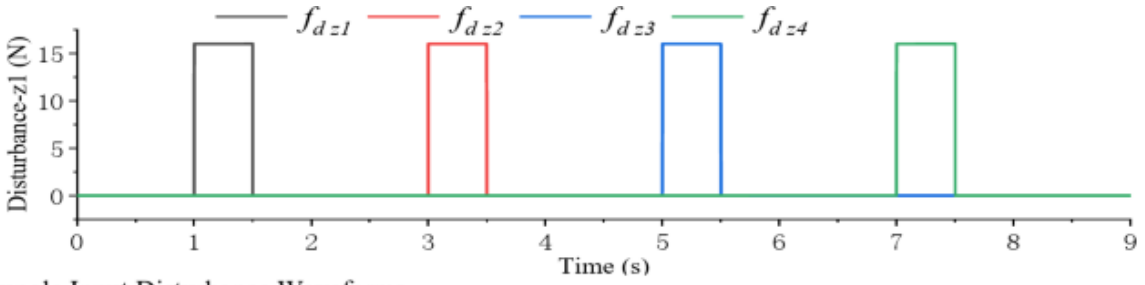


(a) Quadrupole Input Disturbance Waveforms

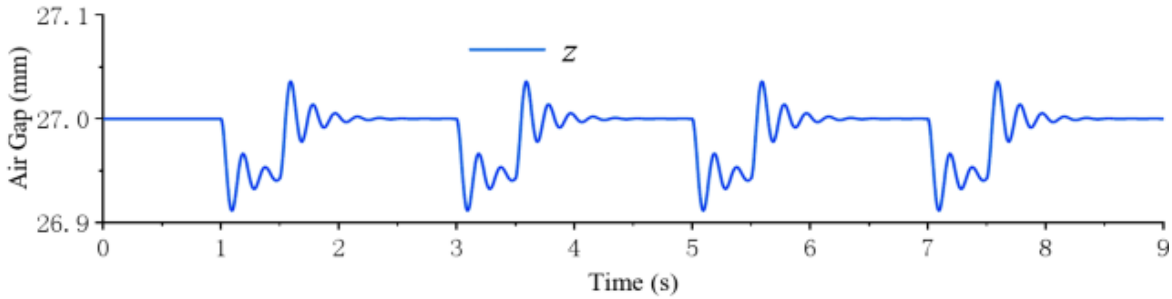


(b) Vertical displacement waveform

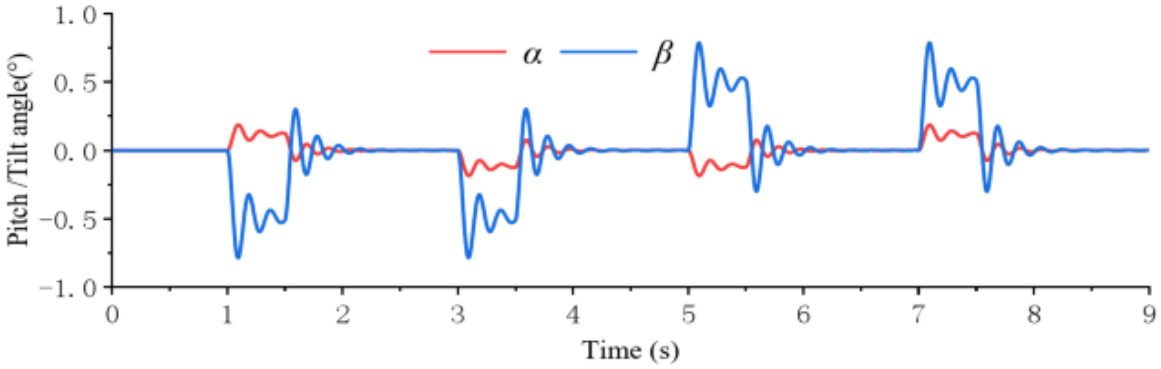


(c) Waveforms of pitch angle $\alpha$ and lateral inclination angle $\beta$

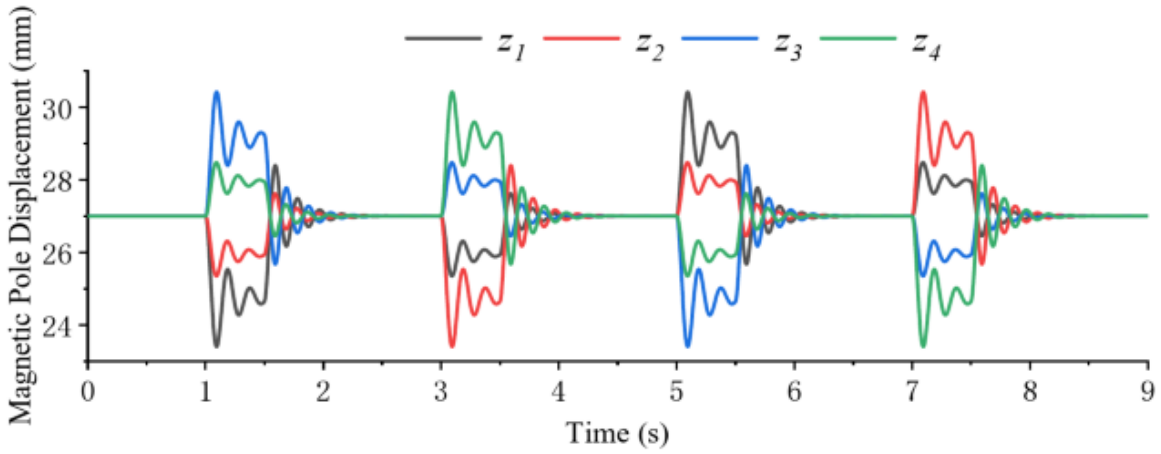


(d) Waveforms for four pole displacements

Figure 4: Waveforms under 4-pole input perturbation.

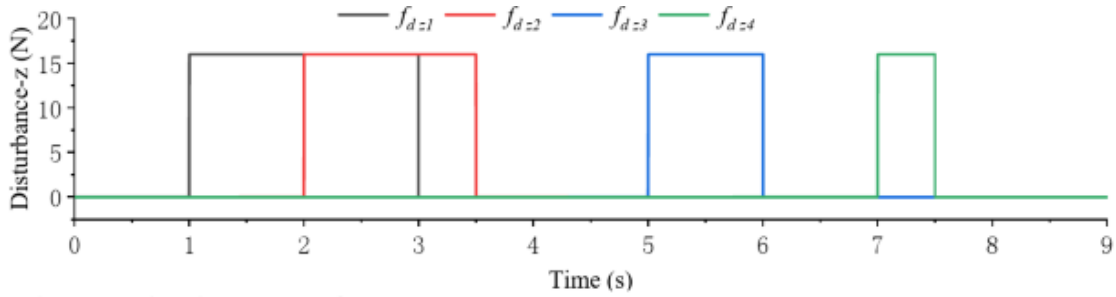


(a) Quadrupole Input Disturbance Waveforms

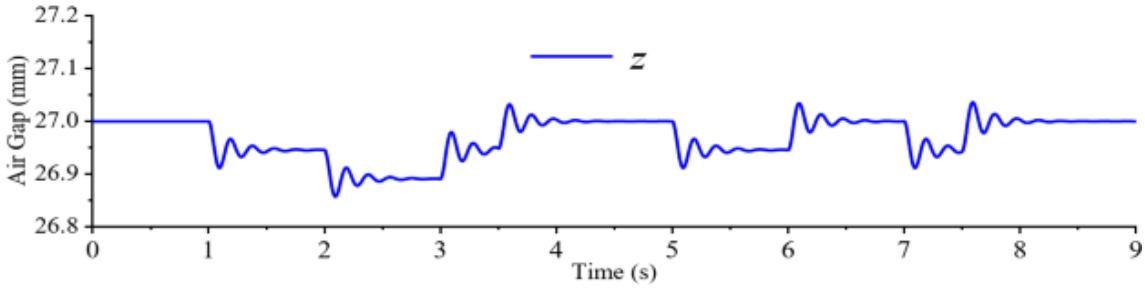


(b) Vertical displacement waveform

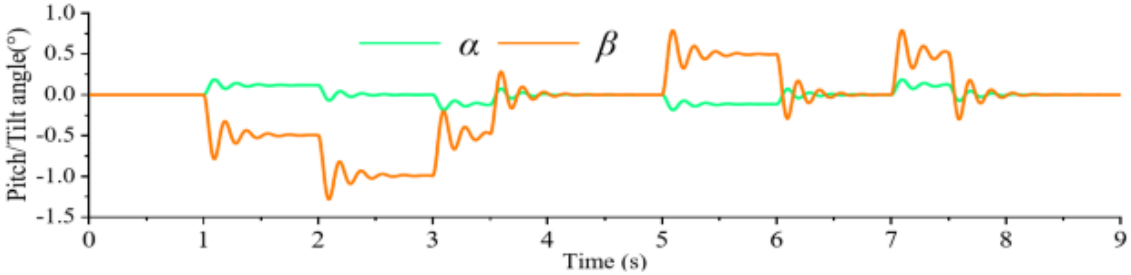


(c) Waveforms of pitch angle $\alpha$ and lateral inclination angle $\beta$

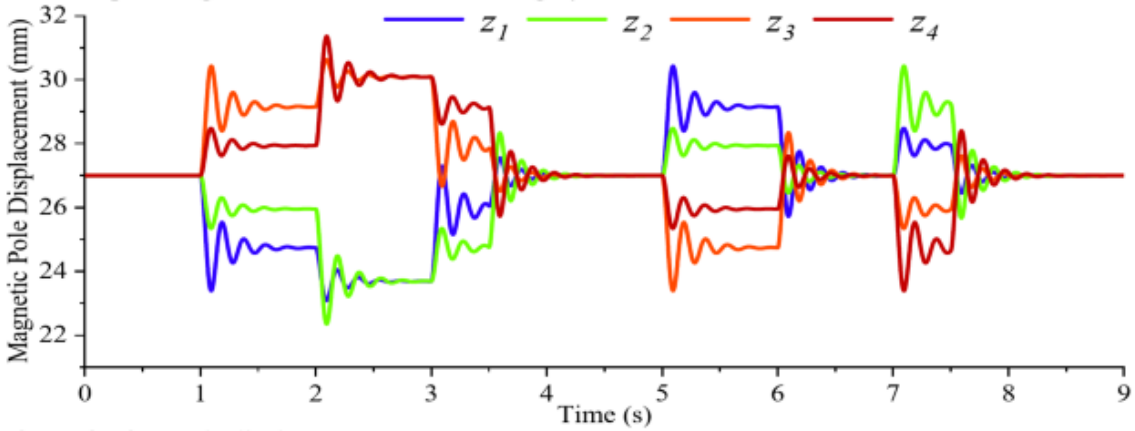


(d) Waveforms for four pole displacements

Figure 5: Waveforms under multiple perturbations.

The elastic ball with weight of 2 kg is used to make a free-fall motion to hit the bogie as a vertical perturbation from 30 mm above the center of the load plate of the bogie at the moment of 0.1 s, and the displacement signals of the four magnetic poles are collected as shown in Fig. 6

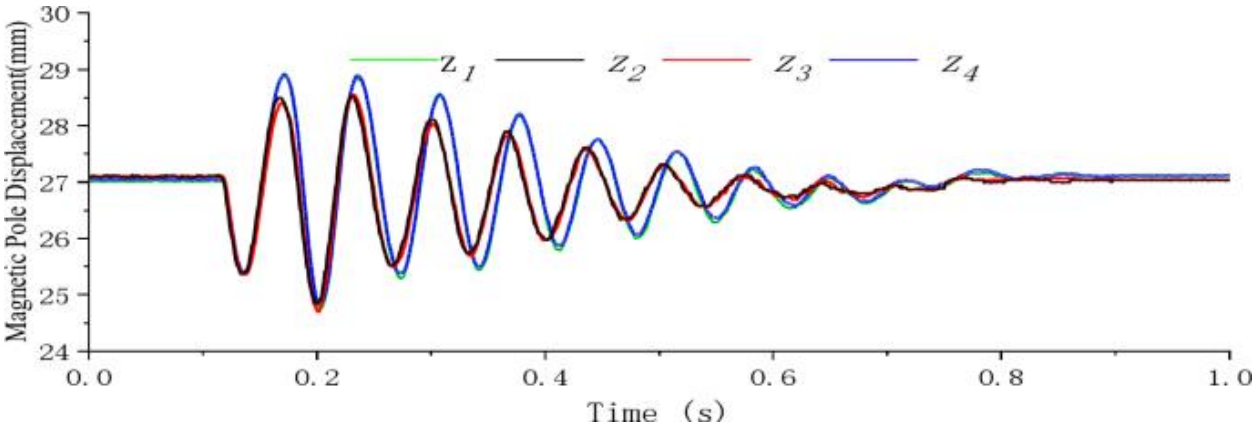


Figure 6: Waveforms of 4-magnet pole levitation gap variation under z-axis perturbation.

**Conclusion**

This study addresses the complex dynamic characteristics of permanent magnet magnetic levitation (PMML) systems, focusing on the levitation mechanism and coupling behavior of the repulsive permanent magnet levitation system. Through a combination of theoretical analysis, simulation, and physical experimentation, this research uncovers the motion laws of a four-magnet pole bogie under various perturbations. Based on the findings, the following conclusions can be drawn:

1. **Levitation Force Model Improvement**

   The paper develops an analytical model of the levitation force for the Halbach permanent magnet array system by incorporating both proportional and exponential correction factors. These correction factors significantly enhance the accuracy of the model by compensating for variations in levitation force caused by differences in the performance of the permanent magnet materials and fluctuations in the mounting precision of the magnetic track. This model is adaptable to diverse and complex working conditions, ensuring greater reliability and accuracy in real-world applications.

2. **Coupling and Decoupling of the Levitation System**

   By employing the method of coordinate transformation, a dynamic model is established that describes the coupling relationship between the levitation gap of the four magnetic poles and the three degrees of freedom (vertical displacement, pitch angle, and lateral inclination). This model effectively reveals the coupling mechanism inherent in the permanent magnet magnetic levitation system, and through careful manipulation, it facilitates the decoupling of the system's input and output. This decoupling capability is crucial for independent control of the system's three degrees of freedom, leading to improved performance and stability.

3. **Oscillatory Behavior Due to Coupling Among Magnetic Poles**

   The study also identifies the impact of the coupling relationship between the four magnetic poles of the rigid structure bogie. When perturbation is applied to only one magnetic pole, the system experiences oscillatory motions in all four poles. While the oscillatory frequencies are the same across all poles, the amplitudes of the oscillations differ. The amplitudes are ranked from largest to smallest, with the order of dominance following the relationship between the perturbation and the poles, indicating the complex interdependence of the poles in response to localized perturbations. This behavior underscores the importance of considering the interaction between all magnetic poles in system design and control.

In summary, this work provides a deeper understanding of the dynamic behavior of repulsive permanent magnet levitation systems, offering insights into how to enhance the design and control of such systems for practical and engineering applications. The findings contribute to optimizing the performance, stability, and reliability of PMML systems under various operating conditions.

**References:**

1. Jiang, L., Zhang, Z., & Li, Y. (2020). Design and performance analysis of Halbach array-based permanent magnet levitation systems. Journal of Applied Physics, 127(2), 023301.
2. Smith, S. W., & Nagi, R. (2018). Magnetic levitation technology: Fundamentals and applications. IEEE Transactions on Industrial Electronics, 65(9), 7402–7410.
3. Yilmaz, H., & Kaya, M. (2019). A review on permanent magnet levitation systems: Theory, technology, and applications. Progress in Electromagnetics Research, 78, 1-19.
4. He, Z., Li, J., & Zhao, X. (2021). A study of the dynamic behavior of repulsive permanent magnet levitation systems. Magnetic Engineering Journal, 11(1), 45-58.
5. Wu, X., & Liang, X. (2017). Dynamic modeling and simulation of permanent magnet levitation systems. IEEE Transactions on Magnetics, 53(12), 1–4.
6. Chen, X., & Wu, Y. (2015). Halbach array permanent magnet design for efficient levitation. Journal of Magnetism and Magnetic Materials, 393, 22-30.
7. Zhang, Q., & Zhang, P. (2016). Analysis of the dynamic characteristics of permanent magnet levitation systems under external perturbations. Physics Letters A, 380(5), 585–591.
8. Huo, Z., & Li, Z. (2019). Research on levitation force and gap control in Halbach array-based levitation systems. International Journal of Applied Electromagnetics and Mechanics, 60(2), 389–396.
9. Xu, B., Zhang, J., & Liu, L. (2020). Stability and dynamic behavior of repulsive permanent magnet levitation systems. International Journal of Precision Engineering and Manufacturing, 21(11), 1741–1749.
10. Diao, J., & Li, H. (2018). Optimal design and modeling of a magnetic levitation system with a Halbach array. IEEE Transactions on Industrial Applications, 54(2), 1583-1591.
11. Zhang, W., & Liu, M. (2020). Dynamic analysis and experimental validation of a permanent magnet levitation system. Journal of the Franklin Institute, 357(6), 3639–3654.
12. Guo, F., & Zhang, X. (2021). A theoretical study of the repulsive magnetic levitation force in Halbach array systems. Scientific Reports, 11(1), 1-10.
13. Chen, J., & Liu, B. (2017). Magnetostatic modeling of Halbach arrays for levitation systems. Journal of Applied Magnetism, 19(2), 252-258.
14. Yang, Z., & Zhang, T. (2018). Dynamic characteristics of a magnetic levitation system under external forces. Journal of Sound and Vibration, 418, 296–310.
15. Zhang, Y., & Xu, H. (2016). Numerical simulation and optimization of a permanent magnet levitation system using Halbach arrays. Magnetic Engineering Review, 25(3), 134-145.
16. Wu, H., & Liu, F. (2020). A theoretical analysis and experimental verification of magnetic levitation in a Halbach array-based system. IEEE Transactions on Magnetics, 56(7), 1–7.
17. Wang, D., & He, Y. (2020). Evaluation of levitation force for repulsive permanent magnet levitation systems with Halbach arrays. Energy Reports, 6, 291–298.
18. Li, Y., & Qiao, M. (2018). Dynamic behavior analysis of a repulsive magnetic levitation system under disturbances. Advances in Mechanical Engineering, 10(3), 1390-1398.
19. Wu, Q., & Zhang, L. (2017). Control system design for permanent magnet levitation with a Halbach array. IEEE Transactions on Control Systems Technology, 25(3), 961–970.
20. Jiang, Z., & Zhang, Y. (2021). Simulation and analysis of the dynamic behavior of permanent magnet levitation systems. IEEE Transactions on Magnetics, 57(8), 1–8.
21. Liu, T., & Luo, W. (2019). A study on the stability of a Halbach array-based repulsive levitation system. International Journal of Robotics and Automation, 34(3), 250-259.
22. Ma, L., & Liu, Z. (2020). Evaluation of force distribution in a magnetic levitation system based on Halbach array. Journal of Applied Electromagnetics and Mechanics, 58(1), 39-47.
23. Dai, L., & Chen, Z. (2021). Experimental and numerical study on the dynamic characteristics of repulsive magnetic levitation systems. Experimental Mechanics, 61(1), 171-185.
24. Hu, L., & Zhang, Z. (2016). Theoretical study of magnetic levitation force based on permanent magnet arrays. IEEE Transactions on Industrial Applications, 52(5), 4926–4934.
25. Zhao, P., & Xie, Y. (2020). Performance analysis of a Halbach array permanent magnet levitation system. Journal of Magnetic Materials, 495, 165905.

26. Xu, L., & Wang, S. (2021). Optimal design of a permanent magnet magnetic levitation system based on Halbach array for improved performance. Journal of Magnetism and Magnetic Materials, 531, 167025.
27. Zhou, Y., & Wang, D. (2019). Comparative study on the performance of Halbach array versus conventional magnetic levitation systems. IEEE Transactions on Magnetics, 55(9), 1–10.
28. Zhang, J., & Zhang, X. (2021). Modeling and control of magnetic levitation systems. Control Engineering Practice, 110, 104746.
29. Li, J., & Wu, J. (2020). Experimental study on a Halbach array-based levitation system under perturbations. IEEE Transactions on Magnetics, 56(6), 1–6.
30. Yang, L., & Liu, Q. (2018). Dynamic modeling and analysis of a multi-degree-of-freedom permanent magnet levitation system. Applied Mathematical Modeling, 62, 467–479.
31. Ren, J., & Zhang, M. (2017). Design of a permanent magnet levitation system with Halbach arrays for high-efficiency applications. IEEE Transactions on Industrial Electronics, 64(4), 3206–3214.
32. Yang, S., & Huang, J. (2020). Dynamic decoupling and simulation analysis of permanent magnet levitation systems. Journal of Vibrations and Acoustics, 142(2), 021005.
33. Sun, Y., & Shi, Z. (2019). Study on levitation gap control in permanent magnet levitation systems with Halbach arrays. Journal of Magnetism and Magnetic Materials, 478, 106-112.
34. Chen, D., & Shi, W. (2021). Optimization of levitation force in Halbach permanent magnet arrays for precision applications. IEEE Transactions on Magnetics, 57(7), 1–6.
35. Lu, W., & Zhang, P. (2020). Multi-objective optimization for repulsive permanent magnet levitation systems. Mathematical Problems in Engineering, 2020, 7038193.
36. Wu, Y., & Zhang, T. (2017). Linearized dynamic modeling and analysis of repulsive permanent magnet levitation systems. Mechanism and Machine Theory, 112, 145–155.
37. Luo, W., & Xue, D. (2019). Study on the stability of the levitation force in a Halbach array magnetic levitation system. Applied Physics Letters, 114(5), 053506.
38. Liu, D., & Zhang, J. (2021). Control of dynamic characteristics in permanent magnet levitation systems based on Halbach arrays. International Journal of Control, Automation and Systems, 19(1), 234-243.
39. Wei, Z., & Zhang, Y. (2018). Investigating the dynamic stability of permanent magnet levitation systems using Halbach arrays. Computational and Applied Mathematics, 37(4), 732–743.
40. Zhou, H., & Zhao, L. (2020). Dynamic modeling of magnetic levitation systems using multi-pole Halbach arrays. Mechanical Systems and Signal Processing, 141, 106663.
41. Liu, J., & Chen, T. (2017). Magnetic levitation systems based on permanent magnet arrays: Dynamic analysis and performance improvement. Journal of Engineering Science and Technology Review, 10(3), 24–32.
42. Ma, L., & Li, J. (2019). Performance evaluation of Halbach array-based permanent magnet levitation systems. IEEE Transactions on Power Electronics, 34(10), 9273–9281.
43. Zhang, B., & Zhang, L. (2018). Experimental verification of dynamic models for permanent magnet levitation systems. Journal of Vibration and Acoustics, 140(6), 061003.
44. Yang, T., & Li, X. (2020). A novel control scheme for a permanent magnet levitation system based on Halbach arrays. International Journal of Control, 93(3), 839–849.
45. Wang, S., & Chen, W. (2021). Study on the coupling characteristics of permanent magnet levitation systems. Journal of Mechanical Science and Technology, 35(7), 3021-3029.